Induction of cortical endoplasmic reticulum by dimerization of a coatomer-binding peptide anchored to endoplasmic reticulum membranes

Grégory Lavieu[a,1], Lelio Orci[b], Lei Shi[a], Michael Geiling[c], Mariella Ravazzola[b], Felix Wieland[c], Pierre Cosson[b], and James E. Rothman[a,1]

[a]Department of Cell Biology, Yale University School of Medicine, New Haven, CT 06520; [b]Department of Cell Physiology and Metabolism, Centre Medical Universitaire, CH1211 Geneva 4, Switzerland; and [c]Biochemistry Center, Heidelberg University, D-69120 Heidelberg, Germany

Contributed by James E. Rothman, March 2, 2010 (sent for review February 21, 2010)

Cortical endoplasmic reticulum (cER) is a permanent feature of yeast cells but occurs transiently in most animal cell types. Ist2p is a transmembrane protein that permanently localizes to the cER in yeast. When Ist2 is expressed in mammalian cells, it induces abundant cER containing Ist2. Ist2 cytoplasmic C-terminal peptide is necessary and sufficient to induce cER. This peptide sequence resembles classic coat protein complex I (COPI) coatomer protein-binding KKXX signals, and indeed the dimerized peptide binds COPI in vitro. Controlled dimerization of this peptide induces cER in cells. RNA interference experiments confirm that coatomer is required for cER induction in vivo, as are microtubules and the microtubule plus-end binding protein EB1. We suggest that Ist2 dimerization triggers coatomer binding and clustering of this protein into domains that traffic at the microtubule growing plus-end to generate the cER beneath the plasma membrane. Sequences similar to the Ist2 lysine-rich tail are found in mammalian STIM proteins that reversibly induce the formation of cER under calcium control.

The current view of the yeast endoplasmic reticulum (ER) discriminates perinuclear ER from cortical ER (cER), which forms a circular structure apposed to the plasma membrane (PM) (1). Both structures are connected by tubulated membranes (2, 3), at least transiently, because ER membranes undergo continuous fission and fusion events (4, 5). cER is a much less prominent feature of most mammalian cells (6). The best-characterized function of cER is its role in the store-operated calcium entry, an ubiquitous Ca^{2+} influx pathway activated in response to depletion of intracellular calcium stores (7).

Ist2 is a "yeast peripheral" protein involved in osmotic stress tolerance. It was initially believed to be located at the plasma membrane (8–11), and its cytosolic tail (Ist2ct) has been shown to carry the peripheral targeting signal (8). Ist2ct includes a dimerization domain (amino acids 878–928) and a lysine-rich carboxy terminal tail containing a KKXX-like motif that has been proposed to interact with the PM (11, 12). The nature of the peripheral Ist2 resident sites remains a matter of debate, however. It was once thought that Ist2 reached the PM in a new Golgi-independent manner (10), but more recently it has been concluded that the major residence site is in fact the cER (11).

To gain insight into the biogenesis of cER in mammalian cells, we investigated whether Ist2, when expressed in a heterologous system, can serve as a useful marker for this compartment. Interestingly, enrichment of Ist2 chimeric protein at the cER appears to directly modulate the formation and/or maintenance of this ER subdomain. These dynamic changes in peripheral ER structure are absolutely dependent on both microtubules and coat protein complex I (COPI) and suggest a different role of COPI than its classical one.

Results

Ist2 Promotes cER Formation. The last two transmembrane domains and the cytosolic tail of Ist2 (Ist2ct) fused to the carboxy terminal extremity of CFP (CFP-Ist2) were expressed in HeLa cells. Confocal microscopy revealed CFP-Ist2 localized at the cell periphery (Fig. 1*C*), consistent with previous reports (13, 14). To further characterize the localization of the transmembrane protein harboring the Ist2 cytosolic tail (TMD-Ist2ct), we generated two stable normal rat kidney (NRK) cell lines, one expressing CD8-GFP, known to be expressed at the cell surface (15), and the other expressing CD8-GFP-Ist2ct. Analysis of the GFP signal by confocal microscopy revealed that both proteins were localized at the cell periphery, but immunofluorescence against the luminal domain of CD8 in non-permeabilized cells showed that only CD8-GFP was exposed to the cell surface (Fig. 1*A*). This result was confirmed by cell surface biotinylation experiments showing that whereas CD8-GFP reacts with nonpermeant sulfonylated biotin, CD8-GFP-Ist2ct and actin do not (Fig. 1*B*). We conclude that the peripheral sites containing CD8-GFP-Ist2ct are distinct from the PM.

CD8-GFP, known to be O-glycosylated in the Golgi (16, 17), appeared as two isoforms, whereas CD8-GFP-Ist2ct appeared as a single species (Fig. 1 *B* and *D*). A jacalin-binding assay revealed that only CD8-GFP underwent Golgi glycosylation (Fig. 1*D*). This is consistent with previous work in yeast suggesting that peripheral Ist2 does not transit through the Golgi (8, 10).

Morphological analysis of cells stably expressing CD8-GFP-Ist2ct by electron microscopy revealed membrane cisternae of various lengths tightly apposed to the PM (mean distance, 6.8 ± 0.4 nm; $n = 81$), decorated with ribosomes on their cytosolic side (Fig. 2 *A–D*). These cisternae were in direct continuity with cytosolic ER cisternae (Fig. S1) and contained BiP, albeit at a lower concentration than cytosolic ER cisternae (Fig. 2 *G–H*). Immunogold labeling revealed that CD8-GFP-Ist2ct was more highly concentrated in these ER subdomains than in cytosolic ER cisternae (Fig. 2 *E* and *F* and Table S1). This type of cER cisternae was hardly observed in WT NRK cells or in cells stably expressing CD8-GFP, in which the chimeric protein was confirmed to be exposed to the cell surface (Fig. S2). These results indicate that Ist2ct not only localizes to, but also induces the formation and/or maintenance of, these yeast-like cER cisternae in NRK cells.

COPI Is Required for cER Induction. COPI is a seven-subunit complex involved in both intra-Golgi and Golgi-to-ER vesicle-mediated trafficking (18, 19). We noticed that Ist2ct harbors a "KKXX-like motif" known to interact with COPI that promotes cargo retrieval from the Golgi to the ER (20). To investigate potential involve-

Author contributions: G.L., L.O., F.W., P.C., and J.R. designed research; G.L., L.O., M.G., M.R., and P.C. performed research; G.L. and L.S. contributed new reagents/analytic tools; G.L., L.O., M.G., F.W., P.C., and J.R. analyzed data; and G.L., L.O., M.G., F.W., P.C., and J.R. wrote the paper.

The authors declare no conflict of interest.

Freely available online through the PNAS open access option.

[1]To whom correspondence may be addressed. E-mail: james.rothman@yale.edu or gregory.lavieu@yale.edu.

This article contains supporting information online at www.pnas.org/cgi/content/full/1002536107/DCSupplemental.

www.pnas.org/cgi/doi/10.1073/pnas.1002536107

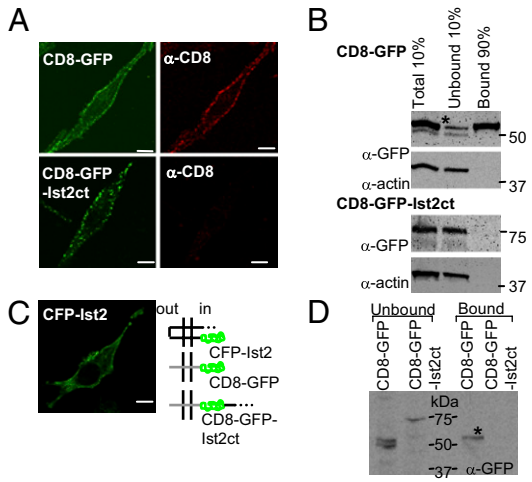

Fig. 1. Ist2ct triggers peripheral localization but not cell surface exposure. (*A*) NRK cells stably expressing CD8-GFP or CD8-GFP-Ist2ct (full-length CD8 fused to Ist2 cytosolic tail) were prepared for immunofluorescence against the extracellular domain of CD8, without previous permeabilization. (Scale bar: 10 μm.) (*B*) After incubation of cells with nonpermeant sulfo-NHS-biotin, lysates from cells expressing CD8-GFP or CD8-GFP-Ist2ct were applied to NeutrAvidin agarose beads. The different fractions were tested by immunoblot analysis for GFP and actin. *Glycosylated form of CD8-GFP. (*C*) HeLa cell transiently expressing CFP-Ist2 (the last two transmembrane domains and the cytosolic tail). (*D*) Lysates from cells expressing CD8-GFP or CD8-GFP-Ist2ct were applied to jacalin (an α-D galactose–binding protein) agarose beads. Both bound and unbound fractions were examined by immunoblot analysis for GFP. (Scale bar: 10 μm.)

ment of COPI in CFP-Ist2 trafficking, β-COP, a common subunit of all known COPI isoforms was down-regulated using siRNA. The siRNA2 sequence was first validated by Western blot analysis to efficiently down-regulate β-COP expression (Fig. 3*A*). HeLa cells were sequentially transfected with the β-COP-targeted siRNA and a soluble DsRed-encoding plasmid (to identify the siRNA- containing cells), and then with the CFP-Ist2–encoding vector. Confocal microscopy revealed that the typical peripheral labeling of CFP-Ist2 (Fig. 3*B*, white and blue arrows) was abolished in cells with reduced β-COP expression and was replaced by reticulate internal labeling typical of ER (Fig. 3*B*, yellow arrows, and Fig. S3). Similar results were obtained after knockdown of the α-COP subunit of COPI (Fig. S4). These results suggest that COPI is involved in the trafficking of TMD-Ist2ct proteins to cER and in the formation of cER. But COPI could play a different, possibly direct role in promoting the transport of Ist2ct from perinuclear ER to cER, or an indirect role in which it interacts with Ist2ct to ensure Ist2ct retrieval from the Golgi in a classical manner.

To distinguish these potential mechanisms, we generated various TMD-Ist2 protein constructs harboring the Ist2ct WT sequence (Ist2ct) or an exclusive KKXX motif ($Ist2_{KKXX}$), or deleted of the motif (Ist2Δ) (Fig. 3*D* and *E*). We examined the ability of these proteins to interact with COPI using an established in vitro COPI-binding assay (21) and characterized their localizations by confocal microscopy. HeLa cells expressing CFP-$Ist2_{KKXX}$ or CFP-Ist2Δ exhibited a diffuse ER-like pattern (Fig. 3*D* and Fig. S5) distinct from the typical peripheral CFP-Ist2 labeling. The in vitro COPI binding assay revealed that Ist2ct bound the COPI complex exclusively as a dimer, whereas $Ist2_{KKXX}$ bound the complex as a monomer (Fig. 3*E*). As expected, Ist2Δ did not bind the COPI complex. We conclude that the lysine-rich tail of Ist2 is distinct from the canonical KKXX signal, suggesting that COPI plays a direct role in TMD-Ist2ct transport.

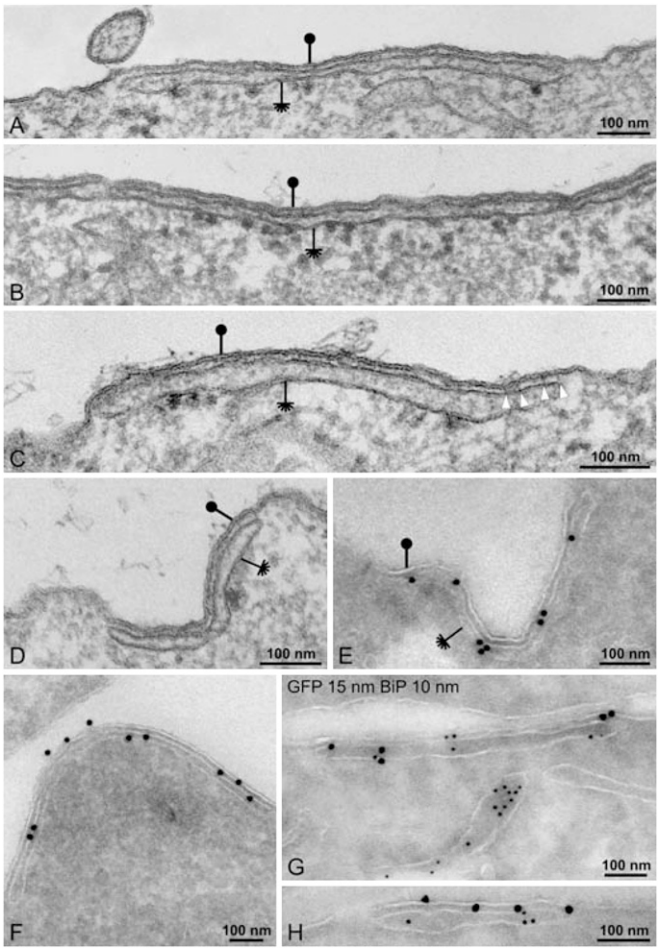

Fig. 2. CD8-Ist2ct promotes cER formation where it localizes. (*A–D*) NRK cells stably expressing CD8-GFP-Ist2 were fixed and processed for Epon embedding, then sectioned and examined by electron microscopy. In these cells, membrane cisternae of various lengths (asterisks) appear tightly apposed to the plasma membrane (full circles). The membrane of cisternae facing the plasma membrane is deprived of ribosomes. A few ribosomes decorate the opposite side of these cisternae and identify them as elements of the rough ER. In some pictures, filamentous elements apparently link the plasma membrane with the ER cisternae (*C*, arrowheads). (*E–H*) Cells expressing CD8-GFP-Ist2 were fixed, processed for cryosectioning, and incubated sequentially with a rabbit antiserum recognizing GFP and with gold-coupled (15-nm particles) goat anti-rabbit antibodies. CD8-GFP-Ist2 was detected primarily in cisternae apposed to the cell membrane (*E* and *F*). Colocalization with BiP (10-nm gold particles) formally identified these cisternae as elements of the ER (*G* and *H*).

Dimerization of the Ist2 Tail Is Required to Induce cER. The findings that Ist2ct binds COPI in vitro exclusively as a dimer suggests that Ist2 dimerization might be required before COPI recruitment and forward transport to cER. This possibility would be consistent with previous studies characterizing residues 878–928 as a domain promoting Ist2p dimerization and required for the transport of Ist2 to the cell periphery (8). To test whether cER induction requires dimerization of this coatomer-binding motif, we drew on a ligand-induced FRB/FKBP dimerization assay (22). We engineered two monomeric fluorescent chimeric proteins containing the last transmembrane domain and the cytosolic tail of Ist2 depleted of the dimerization domain. Each fluorescent chimeric Ist2 protein was fused to FKBP or FRB to generate GFP-$Ist2_{549–878}$-$FKBP_2$-$Ist2_{929–946}$ and Cherry-$Ist2_{549–878}$-FRB-$Ist2_{929–946}$.

HeLa cells expressing both fluorescent monomeric proteins were monitored by confocal microscopy before and during treat-

CELL BIOLOGY

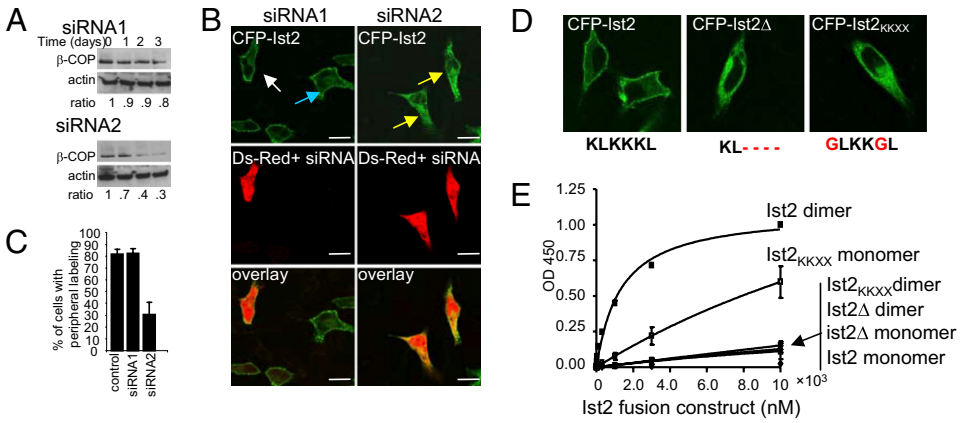

Fig. 3. COPI is required for Ist2 trafficking. (*A*) Lysates of HeLa cells transfected with siRNA targeting the β-COP subunit were tested by immunoblotting for β-COP and actin to evaluate siRNA efficiency. Densitometry was performed using ImageJ software, with β-COP:actin ratio in controls set to 1. (*B*) HeLa cells sequentially transfected with siRNA/DsRed and with CFP-Ist2– encoding vectors were prepared for confocal microscopy. Yellow arrows indicate the intracellular localization of CFP-Ist2 in cells containing the efficient siRNA2, and white and blue arrows show the typical peripheral labeling of CFP-Ist2 in cells containing the nonefficient siRNA1 or expressing CFP-Ist2 alone, respectively. (Scale bar: 10 μm.) (*C*) Graph showing the percentage of double-transfected cells with peripheral Ist2 labeling. Values are mean ± SD of three independent duplicate experiments. (*D*) HeLa cells transiently expressing CFP-Ist2, CFP-IST2Δ (deleted for the last four amino acids), or CFP-Ist2$_{KKXX}$ were prepared for confocal microscopy. The sequence of each chimeric protein tail is indicated below the picture. (Scale bar: 10 μm.) (*E*) The binding of monomeric and dimeric fusion proteins harboring each Ist2 tail sequence (Ist2$_{WT}$, Ist2$_{KKXX}$, and Ist2Δ) to coatomer from rat liver was tested in a microplate assay. Values are mean ± SD of three independent experiments.

ment with the dimerizing agent (AP21967). Live imaging revealed that chemical-induced dimerization dramatically changed the fluorescent protein localization from a cytosolic ER to a peripheral pattern typical of the cER (Fig. 4*A*). In addition, observation of cells fixed at various time points after the induction of dimerization revealed the existence of an intermediate step (Fig. 4*B*). After 15 min, cells showed a punctuate pattern, suggesting clustering of the dimerized proteins in the ER before transportation to the cell periphery, where cER accumulates.

Microtubules Are Required to Form cER. The oligomerized TMD-Ist2ct accumulated significantly at the cell periphery only after a long delay (45 min to 1 h) before (Fig. 3), suggesting that the TMD-Ist2ct–induced cER formation is more complex than a simple random diffusion through the ER network until the proteins passively reach a preexisting cortical site. Thus, microtubules could be required, because the microtubule plus-end tracking protein family (+TIP), which controls microtubule dynamics, has been implicated in coordinating complex aspects of cell and organelle architecture (23). To examine whether microtubules are involved in TMD-Ist2ct trafficking, we analyzed the effect of nocodazole (a microtubule-disrupting agent) on TMD-Ist2 transport, using the dimerizing assay described above. We found that nocodazole prevented the characteristic peripheral labeling of the dimerized TMD-Ist2ct (Fig. 5*B*), which was replaced by the punctuate pattern, suggesting that neoformed Ist2 clusters accumulate in intracellular ER sites and cannot be transported to the cell periphery.

Because end-binding protein 1 (EB1) has recently emerged as a key regulator of dynamic +TIP interaction networks at growing microtubule ends (24, 25), we investigated the consequences of EB1 silencing on TMD-Ist2ct trafficking. We used shRNAs (sh1–3) targeted against EB1 to down-regulate its expression. Western blot

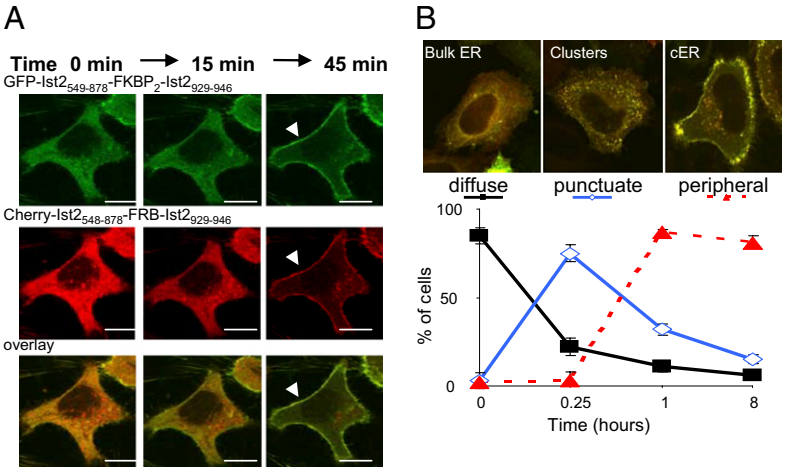

Fig. 4. Ist2ct-induced cER formation requires Ist2 dimerization and Ist2 clustering. (*A*) Live HeLa cells expressing fluorescent transmembrane monomeric Ist2 proteins (GFP-Ist2$_{548–878}$-FKBP$_2$-Ist2$_{929–946}$ and Cherry-Ist2$_{548–878}$-FRB-Ist2$_{929–946}$) were monitored by confocal microscopy. A rapamycin analog (AP21967; 250 nM) was used to trigger protein dimerization. (Scale bar: 10 μm). (*B*) Cells expressing the inducible fluorescent dimers were fixed at different time points after induction of dimerization and analyzed by confocal microscopy. Pictures show the merged fluorescent signals and illustrate the three patterns observed. The graph indicates the percentage of cells exhibiting each pattern over time. Values are mean ± SD of three independent duplicated experiments.

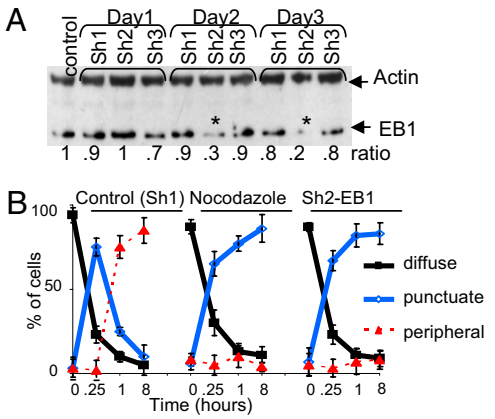

Fig. 5. Microtubules and EB1 are involved in cER formation. (*A*) Lysates from HeLa cells transfected with three different shRNAs against EB1 were tested by immunoblot analysis for EB1 and actin. Silencing efficiency was determined using densitometry. (*B*) Two days after cotransfection, HeLa cells expressing fluorescent monomeric Ist2 chimeric proteins transfected with or without the efficient shRNA against EB1 (Sh2) were monitored by confocal microscopy at different time points after induction of dimerization. When necessary, nocodazole was used at 1 μg/mL 3 h before and during the dimerization procedure. The time course of cER formation was evaluated as described above. Values are mean ± SD of three independent duplicated experiments.

analysis revealed that sh2-encoding plasmid significantly reduced EB1 expression over 3 days (Fig. 5*A*). Two days after transfection, HeLa cells expressing both fluorescent Ist2 monomeric proteins and the shRNAs were monitored by confocal microscopy at various times after the induction of dimerization to examine the time course of cEr formation. Peripheral labeling of cells expressing the multimerized protein was observed in the controls (i.e., cells cotransfected with the inefficient sh1), but was abolished in the cells with reduced EB1 expression (i.e, cells cotransfected with sh2). These latter cells demonstrated an accumulation of intracellular fluorescent clusters (Fig. 5*B*), as is seen in nocodazole-treated cells. We conclude that microtubules, and more specifically EB1, are required for Ist2ct-induced cER formation.

Discussion

We have developed cell assays to investigate the formation of cER in mammalian cells. Our results suggest a simple hypothetical model for the generation of cER in which oligomeric proteins harboring the lysine-rich coatomer-binding tail of Ist2 interact with COPI to form clusters in subdomains of ER membranes. These clusters are transported to the cell periphery at the growing end of the microtubules in an EB1-dependent manner. This model does not address the mechanisms of initial adhesion of the new cortical portions of ER to the inner surface of the plasma membrane.

We note that this pathway shares similarities with the transport of STIM proteins known to reach the ER/PM junction, and may reflect aspects of the trafficking of these proteins (26). The ER-resident STIM proteins act as ER luminal calcium sensors. They multimerize after calcium depletion before being transported to the cell periphery, where they activate a calcium channel (7, 27–29). These proteins harbor a lysine-rich cytosolic tail (29), highly similar to Ist2ct (13), which is required for their peripheral localization. STIM proteins also contain an EB1-interaction domain allowing their targeting to the microtubule plus-end (30). COPI dependency has not been reported for these proteins, however.

The unexplained COPI involvement described in yeast cER inheritance (3) can now be understood. The requirement for COPI is not related to its established role in retrograde transport. A role for COPI in connection with ER is surprising, because coatomer prominently localizes to Golgi membranes but is not a significant morphological feature of ER membranes. But coatomer has been reported to promote vesicle budding from ER membranes in vitro (31) and to be localized to certain ER subdomains in mammalian cells (32). One possibility is that along with its classical role in vesicle formation, the multimeric network of coatomer could be involved in the clustering of proteins in subdomains of ER membranes without vesicle budding. Seedorf et al. (12) reported that the lysine-rich domain of Ist2ct can bind to $PIP(4,5)_2$-containing membranes, and proposed that Ist2ct might act as a bridge between PM and cER structures; however, the amount of peripheral Ist2 in cells with reduced PIP_2 is affected only moderately. Such a role is not incompatible with the COPI binding that we describe herein, assuming that the two events are sequential and that coatomer binding occurs first.

We have demonstrated that cER formation is dynamic and requires microtubules. This is not surprising, given that microtubules are broadly involved in ER dynamics in higher eukaryotes. The fact that EB1 is involved in the formation of Ist2-induced cER suggests that ER subdomains containing Ist2ct attach to the microtubules' growing ends. Further investigation is needed to clearly establish whether Ist2 binds EB1 directly and acts as a microtubule plus-end tracking protein rather than using an ATPase motor for transport. Perhaps a plus-end tracking mechanism is dedicated to cER generation, whereas motor proteins are involved in other aspects of ER dynamics. Of note, peripheral ER organization is normal in kinesin knockout cells (33).

An interesting historical note is the connection between COPI and microtubules. The protein known as β-COP, a subunit of coatomer, was originally described as a microtubule-associated protein. In vitro studies established that β-COP can interact with taxol-stabilized microtubules in a membrane-free system (34). The well-established role of COPI in vesicle-mediated trafficking obscured the possible microtubule-related function of β-COP; however, our findings revive this possibility, and also suggest that the requirement of COPI for cER generation might be directly related to microtubules.

Experimental Procedures

Materials. HeLa and NRK cells were purchased from American Type Culture Collection. Rapamycin analog 21967 and pC4 expression vectors were provided by ARIAD. Jacalin agarose beads and digitonin were purchased from Sigma-Aldrich. NeutrAvidin beads and EZ-Link-Sulfo-NHS-SS-biotin were purchased from Pierce. Antibodies were purchased from Chemicon International (actin and calnexin) and Bioscience (mouse anti-EB1 and anti-CD8 clone Rpa-T8). Antibody against beta-COP (M3A5) previously purified in our lab was used (34, 35). Lipofectamine 2000, DMEM, and FBS were purchased from Invitrogen. siRNAs against β-COP [antisense sequence, 5′→3′ siRNA1 CACUAAUGUCCCAGCAGCUUCAUAU(UU), siRNA2 CAGCUGAAACUGAUCUUCCUUGCAG(UU)] were purchased from IDT. siRNA against α-COP was a gift from W. Nickel (Dharmacon; ref 146404). ShRNAs against EB1 (TRCNO-12226, -12227, and —62142, corresponding to sh1, 2, and 3, respectively) were purchased from Open Biosystems.

Methods. ***Plasmids.*** All of the generated plasmids were based on the pC4 vectors provided by ARIAD, which contained FKBP and FRB sequences flanked at each extremity by XbaI and SpeI restriction sites (http://www.ariad.com/pdf/Reg_Heterodimerization.pdf). Fusion proteins were created making use of XbaI/SpeI compatibility to sequentially introduce the coding sequence of interest (with or without a stop codon) at the required extremity. When necessary, FKBP and FRB sequences were removed before ligation. Thus, pC4-CFP-Ist2 was created, encoding the last two transmembrane domains and the cytosolic tail of Ist2 (amino acids 490–946). For the last insertion of Ist2, a BamH1 restriction site was used, because Ist2 contains a SpeI restriction site. For pC4-CFP-Ist2Δ, the last four amino acids were removed by introducting a premature stop codon by PCR. For pC4-CFP-$Ist2_{KKXX}$, the original sequence Ist2 KLKKKL was mutated into GLKKGL using the QuickChange Site-Directed Mutagenesis Kit (Qiagen). We created pC4-CD8-GFP and pC4-CD8-GFP-Ist2ct, encoding the last 69 amino acids of the Ist2 tail (amino acids 878–946), along with pC4-GFP-$Ist2_{549–878}$-$FKBP_2$-$Ist2_{929–946}$ and pC4-Cherry-$Ist2_{549–878}$-FRB-$Ist2_{929–946}$, both encoding for the last transmembrane domain and cytosolic tail of Ist2 depleted of the dimerization domain. CFP, GFP, and Cherry were amplified from plasmid purchased from Clontech. CD8-GFP was amplified

from a plasmid donated by M. Philips (36). pCJ097 encoding the last 456 amino acids of Ist2 was a gift from M. Seedorf (8). The plasmid encoding NLS-YFP was purchased from Clontech.

For the in vitro binding assay, the fusion proteins were constructed as described previously (21), using cDNAs encoding the cytoplasmic tail of interest beginning from the −15 position of the WT. After insertion of these cDNAs in the pET-32-Xa/LIC plasmid (Novagen), cDNAs were obtained encoding thioredoxin fused to a His tag, followed by an S tag and the cytoplasmic tail of interest. For the dimeric fusion proteins, the codon for proline at position −14 was changed to a cysteine.

Cell Culture, Transfection, and siRNA. HeLa and NRK cells were maintained at 37 °C in 5% CO_2 in DMEM, supplemented with 10% FBS. Cells were transfected using Lipofectamine 2000 (Invitrogen), as recommended by the manufacturer. In brief, 4×10^4 cells/well were plated per 24-well plate. One day later, 0.5 μg of plasmid and 1 μL of lipofectamine were suspended in opti-MEM and added to the cell culture medium for 6 h. After the medium was removed, cells were incubated for at least 24 h in fresh culture medium. All siRNA sequences are "dicer substrate RNAi duplexes," designed by IDT, except the siRNA against the α subunit of COPI (a gift from W. Nickel). A final siRNA concentration of 10 nM was used for silencing. When sequential transfections were required, cells were first transfected with siRNA and DsRed vectors, then HeLa cells were transfected with CFP-Ist2 1 day later. This procedure allowed us to selectively investigate the fate of the cargos in cells containing already active siRNA identified with the DsRed fluorescent signal.

For generation of stable cell lines, NRK cells were cotransfected with pCDNA3.1/hyg (Invitrogen) and pC4-CD8-GFP or pC4-CD8-GFP-Ist2ct. One day later, the cells were split in 10-cm dishes and maintained for 2 weeks in medium containing 100 μg/mL of hygromycin (Gibco). GFP-positive clones were picked and amplified.

Cell Surface Biotinylation, SDS/PAGE, and Western Blot Analysis. These experiments were performed as described previously (37, 38) with slight modifications, as described in *SI Experimental Procedures*.

Lectin Precipitation. NRK cells expressing CD8-GFP or CD8-GFP-Ist2ct were detached and collected for lysate preparation, as described above. Equal amount of protein from each lysate were incubated with 100 μL of jacalin at 4 °C overnight. Samples were centrifuged, supernatants were collected, and the jacalin beads were washed and eluted with the SDS sample buffer. Both fractions were analyzed by Western blotting as described previously (37).

Confocal Imaging. HeLa or NRK cells were grown on glass coverslips in 24-well plates. Cells were fixed for 10 min with 4% PFA. PM was stained using Alexa Fluor 594–labeled cholera toxin β on nonpermeabilized cells. ER was labeled by indirect immunoflurescence against calnexin and an Alexa Fluor 633–coupled secondary antibody after cell permeabilization with 0.1% Triton X-100 and saturation with 1% BSA. CD8 cell surface exposure of nonpermeabilized cells was detected using an antibody raised against the extracellular domain of CD8 (clone Rpa-T8) and an Alexa Fluor 633–coupled secondary antibody. Images were acquired using a confocal microscope (Leica TCS SP2) at 63× magnification, along with the accompanying software package.

Electron Microcopy. For conventional electron microscopy, cell cultures were fixed with 2% glutaraldehyde, buffered with 0.1 M sodium phosphate (pH 7.4), detached from their substrate, postfixed with osmium tetroxide, stained with uranyl acetate (39), dehydrated in ethanol, and embedded in Epon. For immunoelectron microscopy, cells were fixed with 2% paraformaldehyde and 0.2% glutaraldehyde and processed for cryoultramicrotomy, as described previously (40). Ultrathin frozen sections were then prepared and incubated for immunolabeling (41).

The primary antibodies were affinity-purified rabbit polyclonal anti-GFP and mouse monoclonal anti-Grp78/BiP antibody (StressGen Biotechnologies). The anti-GFP antibody was diluted to 1:50 and labeled with goat anti-rabbit IgG gold (gold size, 15 nm). The anti-BiP antibody was used at a 1:20 dilution and was labeled with goat anti-mouse IgG gold (gold size, 10 nm). The labeling densities of GFP and BiP were evaluated using QWin Standard image analysis software (Leica) and a Wacom graphic pen tablet on electron micrographs at a final magnification of 93,500×. The density of the BiP (resp. GFP) labeling was expressed as the number of gold particles per μm^2 (resp. μm) of ER.

Protein Expression, Purification, and Binding Assay. Monomeric thioredoxin fusion proteins were expressed in BL21star cells (Invitrogen), and dimeric fusion proteins were expressed in *E. coli* origami2 cells (Novagen) and purified as described previously (21). The binding assay also was performed as described previously (21). See *SI Experimental Procedures* for more details.

ACKNOWLEDGMENTS. We thank ARIAD Pharmaceuticals for providing us with its regulation heterodimerization kit reagent, and Walther Nickel, Mark Philips, and Matthias Seedorf for providing the reagents used in this study. We thank Ariane Widmer and Marie T. E. Malek for technical assistance, Nadine Dupont for image processing, the Pole Facultaire de Microscopie Ultrastructurale at the University of Geneva Medical School for access to their electron microscopy equipment, Franck Adolf for independently reproducing binding experiments, and Thomas Melia, Rainer Beck, and Stuart Moore for reading the manuscript. This research was supported by a postdoctoral fellowship from the Foundation pour la Recherche Medicale (to G.L.), and by grants from the Swiss National Science Foundation (to L.O. and P.C.).

1. Voeltz GK, Rolls MM, Rapoport TA (2002) Structural organization of the endoplasmic reticulum. *EMBO Rep* 3:944–950.
2. Preuss D, et al. (1991) Structure of the yeast endoplasmic reticulum: Localization of ER proteins using immunofluorescence and immunoelectron microscopy. *Yeast* 7: 891–911.
3. Prinz WA, et al. (2000) Mutants affecting the structure of the cortical endoplasmic reticulum in *Saccharomyces cerevisiae*. *J Cell Biol* 150:461–474.
4. Dreier L, Rapoport TA (2000) In vitro formation of the endoplasmic reticulum occurs independently of microtubules by a controlled fusion reaction. *J Cell Biol* 148: 883–898.
5. Patel SK, Indig FE, Olivieri N, Levine ND, Latterich M (1998) Organelle membrane fusion: A novel function for the syntaxin homolog Ufe1p in ER membrane fusion. *Cell* 92:611–620.
6. Shibata Y, Voeltz GK, Rapoport TA (2006) Rough sheets and smooth tubules. *Cell* 126: 435–439.
7. Liou J, et al. (2005) STIM is a Ca^{2+} sensor essential for Ca^{2+}-store-depletion-triggered Ca^{2+} influx. *Curr Biol* 15:1235–1241.
8. Franz A, Maass K, Seedorf M (2007) A complex peptide-sorting signal, but no mRNA signal, is required for the Sec-independent transport of Ist2 from the yeast ER to the plasma membrane. *FEBS Lett* 581:401–405.
9. Jüschke C, Ferring D, Jansen RP, Seedorf M (2004) A novel transport pathway for a yeast plasma membrane protein encoded by a localized mRNA. *Curr Biol* 14:406–411.
10. Jüschke C, Wächter A, Schwappach B, Seedorf M (2005) SEC18/NSF-independent, protein-sorting pathway from the yeast cortical ER to the plasma membrane. *J Cell Biol* 169:613–622.
11. Maass K, et al. (2009) A signal comprising a basic cluster and an amphipathic alpha-helix interacts with lipids and is required for the transport of Ist2 to the yeast cortical ER. *J Cell Sci* 122:625–635.
12. Fischer MA, et al. (2009) Binding of plasma membrane lipids recruits the yeast integral membrane protein Ist2 to the cortical ER. *Traffic* 10:1084–1097.
13. Ercan E, et al. (2009) A conserved, lipid-mediated sorting mechanism of yeast Ist2 and mammalian STIM proteins to the peripheral ER. *Traffic* 10:1802–1818.
14. Kim YM, Brinkmann MM, Paquet ME, Ploegh HL (2008) UNC93B1 delivers nucleotide-sensing toll-like receptors to endolysosomes. *Nature* 452:234–238.
15. Hennecke S, Cosson P (1993) Role of transmembrane domains in assembly and intracellular transport of the CD8 molecule. *J Biol Chem* 268:26607–26612.
16. Nilsson T, Jackson M, Peterson PA (1989) Short cytoplasmic sequences serve as retention signals for transmembrane proteins in the endoplasmic reticulum. *Cell* 58: 707–718.
17. Snow PM, Keizer G, Coligan JE, Terhorst C (1984) Purification and N-terminal amino acid sequence of the human T cell surface antigen T8. *J Immunol* 133:2058–2066.
18. Orci L, et al. (1997) Bidirectional transport by distinct populations of COPI-coated vesicles. *Cell* 90:335–349.
19. Stenbeck G, et al. (1993) beta′-COP, a novel subunit of coatomer. *EMBO J* 12: 2841–2845.
20. Letourneur F, et al. (1994) Coatomer is essential for retrieval of dilysine-tagged proteins to the endoplasmic reticulum. *Cell* 79:1199–1207.
21. Béthune J, et al. (2006) Coatomer, the coat protein of COPI transport vesicles, discriminates endoplasmic reticulum residents from p24 proteins. *Mol Cell Biol* 26: 8011–8021.
22. Pecot MY, Malhotra V (2004) Golgi membranes remain segregated from the endoplasmic reticulum during mitosis in mammalian cells. *Cell* 116:99–107.
23. Akhmanova A, Steinmetz MO (2008) Tracking the ends: A dynamic protein network controls the fate of microtubule tips. *Nat Rev Mol Cell Biol* 9:309–322.
24. Komarova Y, et al. (2009) Mammalian end-binding proteins control persistent microtubule growth. *J Cell Biol* 184:691–706.
25. Vaughan KT (2005) TIP maker and TIP marker: EB1 as a master controller of microtubule plus-ends. *J Cell Biol* 171:197–200.
26. Orci L, et al. (2009) From the cover: STIM1-induced precortical and cortical subdomains of the endoplasmic reticulum. *Proc Natl Acad Sci USA* 106:19358–19362.
27. Brandman O, Liou J, Park WS, Meyer T (2007) STIM2 is a feedback regulator that stabilizes basal cytosolic and endoplasmic reticulum Ca^{2+} levels. *Cell* 131:1327–1339.
28. Luik RM, Wang B, Prakriya M, Wu MM, Lewis RS (2008) Oligomerization of STIM1 couples ER calcium depletion to CRAC channel activation. *Nature* 454:538–542.
29. Park CY, et al. (2009) STIM1 clusters and activates CRAC channels via direct binding of a cytosolic domain to Orai1. *Cell* 136:876–890.
30. Honnappa S, et al. (2009) An EB1-binding motif acts as a microtubule tip localization signal. *Cell* 138:366–376.

31. Bednarek SY, et al. (1995) COPI- and COPII-coated vesicles bud directly from the endoplasmic reticulum in yeast. *Cell* 83:1183–1196.
32. Orci L, et al. (1994) Coatomer-rich endoplasmic reticulum. *Proc Natl Acad Sci USA* 91: 11924–11928.
33. Tanaka Y, et al. (1998) Targeted disruption of mouse conventional kinesin heavy chain, kif5B, results in abnormal perinuclear clustering of mitochondria. *Cell* 93:1147–1158.
34. Allan VJ, Kreis TE (1986) A microtubule-binding protein associated with membranes of the Golgi apparatus. *J Cell Biol* 103:2229–2239.
35. Paek I, et al. (1997) ERS-24, a mammalian v-SNARE implicated in vesicle traffic between the ER and the Golgi. *J Cell Biol* 137:1017–1028.
36. Chiu VK, et al. (2004) Carboxyl methylation of Ras regulates membrane targeting and effector engagement. *J Biol Chem* 279:7346–7352.
37. Lavieu G, et al. (2006) Regulation of autophagy by sphingosine kinase 1 and its role in cell survival during nutrient starvation. *J Biol Chem* 281:8518–8527.
38. Okazaki Y, Ohno H, Takase K, Ochiai T, Saito T (2000) Cell surface expression of calnexin, a molecular chaperone in the endoplasmic reticulum. *J Biol Chem* 275: 35751–35758.
39. Tandler B (1990) Improved uranyl acetate staining for electron microscopy. *J Electron Microsc Tech* 16:81–82.
40. Volchuk A, et al. (2000) Megavesicles implicated in the rapid transport of intracisternal aggregates across the Golgi stack. *Cell* 102:335–348.
41. Liou W, Geuze HJ, Slot JW (1996) Improving structural integrity of cryosections for immunogold labeling. *Histochem Cell Biol* 106:41–58.